Modelling the effect of hydropeaking-induced stranding mortality on Atlantic salmon population abundance

Journal:	*Ecohydrology*
Manuscript ID	ECO-17-0057.R1
Wiley - Manuscript type:	Research Article
Date Submitted by the Author:	n/a
Complete List of Authors:	Hedger, Richard; Norwegian Institute for Nature Research Sauterleute, Julian; Sweco Norge AS Sundt-Hansen, Line; Norwegian Institute for Nature Research Forseth, Torbjørn; Norwegian Institute for Nature Research Ugedal, Ola; Norwegian Institute for Nature Research Diserud, Ola; Norwegian Institute for Nature Research Bakken, Tor
Keywords:	hydropeaking, stranding mortality, density-dependent mortality, Atlantic salmon, population dynamics

Modelling the effect of hydropeaking-induced stranding mortality on Atlantic salmon population abundance

Effect of hydropeaking stranding mortality on Atlantic salmon population abundance

Richard D. Hedger: Norwegian Institute for Nature Research, NO-7485, Trondheim, Norway. richard.hedger@nina.no. +47 40 46 65 68.

Julian Sauterleute: Sweco Norway, NO-7030 Trondheim, Norway; SINTEF, NO-7465 Trondheim, Norway. julian.sauterleute@sweco.no.

Line E. Sundt-Hansen: Norwegian Institute for Nature Research, NO-7485, Trondheim, Norway. line.sundt-hansen@nina.no.

Torbjørn Forseth: Norwegian Institute for Nature Research, NO-7485, Trondheim, Norway. Torbjorn.Forseth@nina.no.

Ola Ugedal: Norwegian Institute for Nature Research, NO-7485, Trondheim, Norway. Ola.Ugedal@nina.no.

Ola H. Diserud: Norwegian Institute for Nature Research, NO-7485, Trondheim, Norway. Ola.Diserud@nina.no.

Tor H. Bakken: SINTEF, NO-7465 Trondheim, Norway. tor.haakon.bakken@sintef.no.

Key words: hydropeaking; stranding mortality; density-dependent mortality; Atlantic salmon; population dynamics

ABSTRACT

Studies of hydropeaking-induced stranding mortality on fish populations have been confined to analysis of empirical data and/or short-term hydraulic-habitat modelling of individual events, and are thus limited as to how they may be used to infer long-term effects in fish populations. In this study, the effects of stranding mortality on an Atlantic salmon population were simulated using an individual-based Atlantic salmon population model with the objective of determining the sensitivity of population dynamics to stranding. It was found that density-dependent mortality (an alternative source of mortality in juvenile Atlantic salmon) partially compensated for stranding mortality, acting as a negative feedback mechanism that dampened change in population abundance. Stranding caused a perturbation in population dynamics, and effects of individual stranding events persisted in time across the life-stages of the population. Effects on population abundance depended on the time of year when stranding was applied, both because of intra-annual changes in stranding mortality probability and because of intra-annual changes in the ability of density-dependent mortality to compensate for stranding mortality. We concluded that empirical measurements of stranding mortality have limited potential for inference of overall effects on the population, and a more dynamic modelling approach, incorporating system feedback, allows for a better modelling of the impact of stranding. Sensitivity analysis showed that population abundance was highly sensitive to density-dependent mortality, and we suggest that this area should be prioritised for further research when investigating the effects of hydropeaking on rivers.

1 Introduction

Hydropeaking is a form of flow regulation used in some regulated rivers which involves initiating frequent, short-term fluctuations in river discharge, executed with the objective of balancing variation in electricity demand through changes in water extraction for powering hydropower turbines (Niu and Insley, 2013). Hydropeaking may detrimentally affect riverine fish populations (Hauer *et al*., 2017b). The reduction in channel discharge that occurs during down-ramping (short-term reduction of water flow in the regulated watercourse, when water is extracted for use in a turbine) may rapidly dewater shallower areas of the channel, which may lead to fish becoming stranded in dewatered areas (Saltveit *et al*., 2001; Tuhtan *et al*., 2012). The risk of this stranding depends on a variety of abiotic and biotic factors including down-ramping speed, season, water temperature, light conditions, fish life-stage and fish behaviour (see Saltveit *et al*., 2001; Halleraker *et al*., 2003; Irvine *et al*., 2009). Stranding may lead to fish mortality, depending on the interaction between the body sizes of the stranded fish, the river bed substrate size, and the length of the stranding event (see Hvidsten, 1985; Bradford, 1997; Nagrodski *et al*., 2012). In countries reliant on hydropower, hydropeaking may be a pertinent issue with respect to the conservation of riverine fish populations. For example, a majority of Norwegian rivers with high Atlantic salmon (*Salmo salar* L.) production are regulated for hydropower, and hydropower regulation has been a major factor in the loss of 19 stocks (NASCO, 2009). Given that Atlantic salmon population abundances are at historically low levels (Chaput, 2012), research in this area is warranted.

Different approaches have been used to determine how hydropeaking may affect fish populations. Field experiments, involving monitoring fish abundances within net pens placed *in situ* in the river, may be used to directly observe stranding mortality, and determine its sensitivity to different aspects of the flow regime or river characteristics (Saltveit *et al*., 2001; Halleraker *et al*., 2003; Irvine *et al*., 2009) but small sample sizes and often low statistical power make it difficult to generalise results. A statistical approach, involving analysing data collected in rivers affected by or free from hydropeaking may be used to examine aggregate effects of hydropeaking (Liebig *et al*., 1999; Schmutz *et al*., 2015), but there is the potential for confounding factors to influence conclusions, and it may be difficult to determine causative pathways as to the manner in which hydropeaking influences fish populations. Hydrodynamic modelling, sometime combined with fish habitat modelling, allows for predicting stranding risk from individual hydropeaking events, and analysing causative relationships under completely controlled conditions (Tiffan *et al*., 2002; Tuhtan *et al*., 2012; Hauer *et al*., 2014). This approach, however, is typically used to model individual or a small number of hydropeaking events, and is limited in regards to the ability for evaluating long-term effects of hydropeaking on fish population dynamics. This is unfortunate because fish populations have complex dynamics: for instance, the increase in fish mortality associated with a stranding event, may reduce fish density, and therefore reduce subsequent density-dependent mortality (an alternative soure of mortality that fish experience; see Einum *et al*., 2006), partially compensating for the stranding event. To model long-term effects of repeated stranding events, some form of population modelling, which incorporates the feedback mechanisms controlling the population, is required.

In this study, we investigate the sensitivity of the population dynamics of Atlantic salmon to hydropeaking-induced juvenile stranding mortality using an individual based model (IBM) approach.

1. We begin with an initial simulation where we examine the effect of hydropeaking-induced stranding mortality on long-term Atlantic salmon population dynamics. We investigate how stranding mortality affects density-dependent mortality (the other source of within-river mortality that is simulated in the model).
2. We then examine the long-term effects of stranding on Atlantic salmon population dynamics to determine how long it takes for the equilibrium population to recover from the perturbation induced by stranding.
3. We then examine the relative sensitivity of the Atlantic salmon population to the seasonal pattern of hydropeaking.
4. Finally, we examine the relative sensitivities of the Atlantic salmon population to different sources of mortality – both hydropeaking-induced stranding mortality and density-dependent mortality – to identify where future research should be focused when trying to predict population effects of hydropeaking.

2 Materials and methods

2.1 Study area

Simulations on the effect of hydropeaking-induced stranding mortality on Atlantic salmon population dynamics were parameterised using data from the River Mandalselva, a large regulated river (length = 115 km, catchment area = 1800 km^2, mean annual discharge = 88 $m^3 s^{-1}$) in Southern Norway (58°2' N, 6°28' E) (see Ugedal *et al.*, 2006). This river was chosen because it is one of the most productive Atlantic salmon rivers in Norway that is subject to hydropeaking, and has comparatively detailed data on river morphometric characteristics, Atlantic salmon population characteristics and flow regulation regime. Hydropower affects salmonid populations within this river through a variety of mechanisms, including stranding, sedimentation of spawning habitat and obstruction of migration, and it has been estimated that the combined effects of hydropower regulation have reduced the total production of smolts (early adults that migrate to sea) by 20 – 40% (Ugedal *et al.*, 2006).

The watercourse downstream of the outlet from the most downstream hydropower station (Laudal hydropower station), comprising a stretch of 19.8 km in length, was modelled. This part of the watercourse has a low gradient (change in elevation = 12 m), and meanders through alternating sections of floodplains and incised valleys. The channel is predominantly composed of glide and walk mesohabitat classes, but there are some rapids. There is a trend in substrate size from stones/gravel in the upper part of the watercourse to fine gravel/sand in the lower part, with areas of coarser substrate being situated where the river is incising through valleys. The channel cross-section is simple, with few islands present, and limited departure from a 'U' to 'V' shaped profile. The ratio between peak and base flow in this stretch is typically between 1.5 and 2, but may be as high as ≈ 5 in extreme situations. Ramping rates during hydropeaking are typically low (mean ≈ 5 cm h^{-1}, max ≈ 10-20 cm h^{-1}).

2.2 Individual based model (IBM)

The Atlantic salmon population was modelled using IB-salmon, a spatially-explicit IBM. This model was developed to simulate Atlantic salmon population abundances across all life-stages over long-term (multi-decadal) periods. It was calibrated using time-series data on population characteristics (including juvenile abundance, smolt production, and size at age) for a salmon-bearing river, the River Nausta in western Norway (Hedger *et al*., 2013a), and has been used to simulate the effects of climate change (Hedger *et al*., 2013b), hydropeaking (Sauterleute *et al*., 2016) and habitat remediation (Bustos *et al*., 2017) on Atlantic salmon populations for several rivers in Norway, including the upper and lower watercourses of the River Mandalselva. It simulates individual Atlantic salmon life-history processes (ontogeny, fecundity, mortality, migration) using heuristic functions derived from field and laboratory experiments. Processes modelled are shown in Hedger et al. (2013a). Life-stages modelled are: (i) *eggs*, deposited in the riverbed substrate; (ii) *fry*, juvenile fish in the week of swim-up from the hatched eggs; (iii) *parr*, juvenile fish from one week after swim-up to the spring several years later when individuals are large enough to smoltify; (iv) *smolts*, early adults that have smoltified (in the process of adapting to salt water so that they may travel to sea); (v) *adults at sea*; and (vi) *returning adults* that have returned to the river to spawn. Only parr and later developmental stages are modelled as individual elements; egg and fry abundance are modelled using a group based approach for the sake of computational efficiency. Freshwater processes (growth, mortality, migration) are modelled with a weekly resolution throughout a watercourse that is longitudinally compartmentalised into 50 m long sections; marine processes are modelled in a spatially-integrated fashion with a yearly resolution. The age group of an individual increases on the first week of the year; for example, age 0+ parr (parr in the year of swim-up) become 1+ parr the first week of the following year.

Parr juveniles are subject to two forms of mortality within the IBM: (i) *density-dependent mortality* resulting from biomass exceeding that which can be supported by the river, and (ii) *hydropeaking-induced stranding mortality*.

(i) Density-dependent mortality is the mortality that occurs when the total biomass of Atlantic salmon parr within a given section of the river exceeds the biomass that can be supported (the carrying capacity, K) of that section. This mortality is termed *density-dependent* because it only occurs when parr densities are high (relative to what can be supported). In the example in Figure 1 (left panel), the carrying capacity of the section (K_{sec}) is 500 g. A total parr biomass below this threshold will not result in density-dependent mortality: for example, a total biomass of 400 g at time T will give a total biomass of 400 g at time T+1. However, when the carrying capacity of the section is exceeded – as a result of recruitment from fry into parr, parr individual body mass growth, parr immigration, and/or a reduction in wetted (water covered) area – biomass surplus to the parr carrying capacity are removed from the section: for example, a total biomass of 800 g at time T will give a total biomass of 500 g (equivalent to the section carrying capacity) at time T+1. Surplus parr are subject to a pre-defined *density-dependent mortality probability*; survivors migrate to a neighbouring section. The default is that all survivors migrate downstream – the probability of a surviving individual migrating downstream equals one – although this may be changed according to simulation. Thus, in the example shown, of the 300 g of surplus parr (the difference between the 800 g at time T and the 500 g carrying capacity), some are killed and some migrate out of the section. Removal of parr surplus to the section carrying capacity is size-independent: that is, parr are selected at random until the carrying capacity is no longer

exceeded. Density-dependent mortality is modelled as a weekly process, so depends on the mean weekly wetted area, which in turn controls the total carrying capacity of the section each week.

(ii) Hydropeaking-induced stranding mortality is the mortality that juvenile fish are susceptible to if they find themselves in a dewatered part of the channel on the down-ramping phase of a hydropeaking event. This is density-independent: that is, the probability of an individual experiencing mortality is independent of the number of conspecifics within the dewatered area. Thus, the abundance within a dewatered area at time T+1 is directly proportional to the number at time T (Figure 1, right panel). Stranding mortality occurs within dewatered areas with every hydropeaking event, so the total probability of an individual experiencing stranding mortality within any given week (*M*) in the IBM simulation is calculated from the assigned stranding mortality probability (*S*), the proportion of the section that is dewatered (A), and the number of stranding events within that week (n) (see Sauterleute *et al.*, 2016):

$$M = 1 - \left(1 - (\mathrm{S} \times \mathrm{A})\right)^{\mathrm{n}} \quad (1)$$

The assigned stranding mortality probability within the IBM may be specified to be dependent on the individual's life-stage (fry; age 0+ parr; and age 1-4+ parr), the diel period and the season. The rationale for developing the model in this way and the selection of stranding mortality probability values were based on field and laboratory experiments (Saltveit *et al*., 2001; Halleraker *et al*., 2003; Harby *et al*., 2004). Potential limitations of this approach are discussed in Section 4.2.

Atlantic salmon smolts migrating to sea experience an initial post-smolt mortality, an annual sea mortality, and an annual probability of returning to the river along with a body size drawn from a pre-set size distribution. Returning adults subsequently deposit eggs, so egg deposition is affected by the history of what has occurred in the river (i.e. juvenile survival).

2.3 Parameterising the model

The watercourse was modelled as a 1-D along-channel profile, separated into sections of 50 m in downstream length, with each section spanning the entire channel. With regard to modelling the Atlantic salmon population, relevant attributes of the watercourse were (i) the location of spawning redds, and the parr carrying capacity per unit area (g m^{-2}), (ii) weekly discharge and water temperature, (iii) wetted area as a function of weekly discharge (which together with parr carrying capacity per unit area determined density-dependent mortality); and (iv) the proportional area dewatered in a stranding event (which affected stranding mortality).

Initial egg deposition across the modelled watercourse was estimated according to the number of redds (nests) in each section, determined from survey data (B. Skår, Uni Miljø), with the assumption that one adult female would deposit eggs in each redd. The parr carrying capacity per unit area was determined directly as a function of substrate size, using habitat survey data (H. M. Berger, Norwegian Institute for Water Research).

An intra-annual pattern of discharge and water temperature was generated using data obtained from a gauge at the outlet of the Laudal hydropower station. This pattern was repeated to produce a 50-year time-series of mean weekly discharge and water temperature. The total amount of habitat available in each section (i.e. how much was submerged) depended upon weekly discharge and the channel profile. Atlantic salmon body mass growth, which affected total biomass and therefore density-dependent mortality, was dependent on weekly water temperature.

Detailed measurements of the along-stream variation in the cross-sectional channel profile have not yet been made for the entire watercourse of the River Mandalselva, and resource limitations prevented us from surveying profiles throughout the entire modelled watercourse. We therefore used an approach of surveying stretches with representative channel types, modelling discharge-wetted width relationships within these stretches using 1-D hydraulic modelling, and then applying modified discharge-wetted width relationships derived from this modelling to the entire modelled watercourse, with modifications based on measurements from aerial photographs. The channel profiles of three representative stretches of the river were surveyed by ground measurement: (1) a stretch of the river with a more 'U' shaped channel (12 cross-sectional profiles measured over a 460 m long stretch); (2) a stretch of the river with an intermediate, slightly more 'V' shaped channel (7 profiles measured over a 325 m long stretch); and (3) a stretch of the river with a more 'V' shaped channel (9 profiles measured over a 450 m long stretch). The relationship between discharge and wetted width for each representative stretch was determined using the 1-D hydraulic model HEC-RAS (Hydrological Engineering Center, US Army Corps of Engineers). This model calculates the 1-D St. Venant equation for open channel flow using a four-point implicit finite difference scheme. The hydraulic model was calibrated using measurements of water level in each profile for a single discharge by varying the roughness. Steady-state simulations at different discharges were then used to establish discharge-wetted width relationships for each representative channel profile. Polynomial regression was then used to produced discharge-wetted width curves from the simulated values (Table 1). Each 50 m long section of the watercourse was then classified into one of the channel profiles from analysis of aerial photographs and bank-side observations, and the maximum wetted width of each section was determined from measurements from aerial photographs (imagery obtained from norgeibilder.no). Wetted width for each 50 m section and each week of the simulation was determined from mean weekly discharge, using the appropriate channel type relationship ('U'-shaped, intermediate of 'V'-shaped), scaled by the ratio between the maximum wetted width of the 50 m section in question and the maximum wetted width of the representative stretch in question.

The proportion of each section that was dewatered during a down-ramping event (minimum discharge at down-ramping = 20 $m^3 s^{-1}$) was determined from linear relationships established between wetted widths measured from aerial photographs taken at different discharges (17 - 27 $m^3 s^{-1}$ and 46 - 51 $m^3 s^{-1}$). This allowed for a proportion of the channel dewatered ranging between 0 and 1 according to section. Hydropeaking events were independent of weekly discharge, and consequently the area dewatered in a hydropeaking events was independent of the weekly wetted area (which was dependent on the weekly discharge).

Wetted areas (for each week and section) were then read by the IBM to determine weekly density-dependent mortality. The proportion of each section that was dewatered in each stranding event and the number of events per week were then used to determine stranding mortality (equation 1).

The objective of this study was to use the selected river as a means by which we could analyse the sensitivity of the population to stranding, and as such, the intent was not to produce an exact simulation of the population within the river. However, simulated abundances and fish sizes were compared with those measured *in situ* to confirm that the model was creating a biologically feasible population. Estimates of parr abundance were obtained from the Norwegian Environment Agency (NVE), based on electrofishing at 7 stations in October/ November, yearly from 2002 – 2010, in the modelled watercourse. Measurements of average fish length according to age group (0+, 1+, 2+ and 3+) were available from the NVE for 1998 – 2001. Estimates of smolt production were obtained from studies by the Norwegian Institute for Nature Research (Ugedal *et al.*, 2006).

2.4 Analysing the effect of hydropeaking

In all simulations, the IBM simulated weekly processes for a period of 50 years. The first ten years were used as a "burn-in" time to generate a full population age distribution. The remaining 40 years were used for analysis of the effect of hydropeaking-induced stranding on the population dynamics. The primary metrics used to quantify this effect on the population were parr abundance and smolt production.

Four sets of simulations were run: (i) simulations investigating the effect of hydropeaking on long-term Atlantic salmon population dynamics, focusing on compensatory changes in density-dependent mortality in response to mortality from stranding; (ii) simulations investigating how long it took for the equilibrium population to recover from the perturbation induced by hydropeaking; (iii) simulations investigating the effect of different seasonal patterns of hydropeaking; and (iv) sensitivity analysis simulations, allowing the relative importance of uncertainty in stranding mortality with respect to density-dependent mortality to be determined.

1) Effect of hydropeaking on long-term population dynamics. Atlantic salmon population abundance was simulated with a hydropeaking regime which involved down-ramping once per day on the weekdays of Monday-Friday (a total of five events per week), with a down-ramped discharge of 20 $m^3 s^{-1}$. Fry stranding mortality probability (S_{fry}) was assigned to be 0.9; parr stranding mortality (S_{parr}) was assigned to be 0.2 (constant across age groups). Values for S_{fry} and S_{parr} were in the mid-range of values presented within the literature (Saltveit *et al*., 2001; Halleraker *et al*., 2003; Harby *et al*., 2004). For comparison, a control scenario was run with no hydropeaking.

2) Population recovery from perturbation induced by hydropeaking. Simulations were run with hydropeaking occurring over a set range of years (1, 2, 3, ... 10) to explore how the recovery of a population on the cessation of hydropeaking was influenced by the length of time over which hydropeaking had been applied. Stranding mortalities and weekly

hydropeaking frequencies were the same as in the initial simulation (S_{fry} = 0.9; S_{parr} = 0.2; five hydropeaking events per week).

3) Population sensitivity to seasonal pattern of hydropeaking. Simulations were run with hydropeaking absent except for at specific-four week periods within the year (week of year 1-4, 5-6, ... 48-52) to determine the seasonal effect of hydropeaking on the population. For each four-week period, two sets of simulations were run: (i) hydropeaking with a fixed stranding mortality probability that was independent of season (S_{fry} = 0.9; S_{parr} = 0.2); and (ii) hydropeaking with a seasonally-dependent stranding mortality (
Table 2). In the latter case, separate simulations were run with seasonally-dependent mortalities consistent with hydropeaking during daytime and hydropeaking during night-time. Assigned seasonally-dependent stranding mortality probabilities were based on information in the literature (Saltveit *et al*., 2001; Halleraker *et al*., 2003; Harby *et al*., 2004). Running simulations with both seasonally-independent and seasonally-dependent mortalities allowed determination of whether seasonal effects on population dynamics were a function of seasonal dependence in stranding mortality probability (e.g. greater parr stranding mortality probability if a stranding event occurred in winter than in summer), or the temporal proximity of the stranding event to the time of smoltification, when juveniles became adults, migrated to sea and were no-longer subject to stranding.

4) Sensitivity analysis: stranding mortality versus density-dependent mortality. A linear sensitive analysis approach was used to determine the sensitivity of smolt production with respect to: (i) stranding mortality probability of fry, 0+ parr and 1-4+ parr, and (ii) density-dependent mortality of parr. With respect to density dependent mortality, two parameters were analysed: density-dependent mortality probability (the probability that surplus parr died); and the probability of a surviving individual migrating downstream. The latter parameter affected subsequent parr density-dependent mortality indirectly by determining total parr biomass in sections of the river that the parr migrated too. For each simulation, the value of the parameter under investigation was modified around the baseline value (
Table 3). The range of values for stranding mortality was based on the range of values that have been established in the literature, although we tested a range of fry stranding mortality probabilities ranging from 0 to 1, reflecting the relative lack of research for this life-stage. Values for density-dependent mortality probability have not been well established so we examined a range from 0.05 (a very low mortality rate for individuals exceeding the carrying capacity) to 1 (all individuals exceeding the carrying capacity experiencing mortality). Values for migration direction have also not been well established, but there is a tendency for individuals to migrate downstream (Beall *et al.*, 1994; Brunsdon *et al.*, 2017). We therefore used a range from 0.5 (50% migrating downstream) to 1 (100% migrating downstream). A linear sensitivity analysis approach was used, rather than a more advanced approach such as Monte Carlo modelling, so as to minimize the number of simulations required to determine sensitivities. This was necessary because of the long run-time required for each simulation.

3 RESULTS

Populations characteristics simulated by the IBM were similar to those observed in terms of overall parr abundance and body length, and smolt production. Mean overall simulated parr abundances were similar to those observed using electrofishing, although the simulated age

distribution was less positively skewed than that observed (Figure 2, left panel). Simulated body lengths were similar to, but slightly larger, than those observed (Figure 2, right panel). Simulated mean smolt productions were 2.84 smolts 100 m^{-2} (no hydropeaking) and 0.51 smolts 100 m^{-2} (five hydropeaking events per week), within the same order of smolt production estimated by Ugedal *et al*. (2006) which ranged from 1.8 – 3.7 smolts 100 m^{-2}. Given the overall similarity between simulated and observed populations, it was concluded that the IBM outputs were satisfactory for investigating the sensitivity of Atlantic salmon population dynamics to stranding mortality.

3.1 Effect of hydropeaking on long-term population dynamics

Hydropeaking (5 events per week) reduced parr abundance and smolt production relative to the control group of no hydropeaking (Figure 3). The percentage reduction in parr abundance from stranding tended to increase with increasing age group. For example, stranding resulted in a ≈38.6% reduction in the abundance of 0+ parr, and a ≈44.2% reduction in the abundance of 3+ parr. However, the overall effect of hydropeaking on the size distribution of the population was small because, whether hydropeaking was applied or not, the parr age structure was so strongly positively skewed (dominated by parr from younger age groups). Stranding resulted in a ≈76.1 % reduction in production of age 2+ smolt, and a ≈78.7% in the production of age 3+ smolt.

The intra-annual pattern of parr abundance with the application of hydropeaking was broadly similar to that in the absence of hydropeaking (Figure 4). In both cases, parr abundances peaked mid-year (week of year ≈ 26) due to recruitment from fry, and then decreased onwards from the summer peak due to density-dependent mortality resulting from the parr carrying capacity being exceeded. Density-dependent mortality rose to an initial peak around week of year 32, largely due to increases in biomass due to somatic growth, but decreased to low levels by week of year 44. Density-dependent mortality only occurred again with the next phase of recruitment into parr the following year. Hydropeaking caused stranding mortality throughout the year, regardless of the density of parr, resulting in a decline in parr abundance. This decline in parr abundance meant that parr carrying capacity was exceeded to a lesser extent, so density-dependent mortality was reduced. Consequently, density-dependent mortality was less in the simulation with hydropeaking than in the simulation without hydropeaking. The effect of stranding on parr abundance was cumulative over successive years, reducing the summer maximum parr abundance by nearly two-thirds after six years of stranding (Figure 5).

3.2 Population recovery from perturbation induced by hydropeaking

The rate of recovery of parr abundance to pre-hydropeaking abundance levels after the cessation of hydropeaking was strongly dependent on the number of years for which hydropeaking was applied (Figure 6, upper panel). For example, with hydropeaking being applied for one year only, parr abundance returned and remained at pre-hydropeaking levels 11 years after cessation of hydropeaking. In contrast, the effect of consistent hydropeaking over a 10 year period was to cause such a reduction in abundance such that the population had still not recovered 20 years after hydropeaking had ceased.

The rate of recovery was not consistent from year to year, particularly if hydropeaking had only been applied for a small number of years. For example, when hydropeaking was applied for one year only, there was a reduction in parr abundance in that year (year 11) due to stranding mortality, but this was followed by a peak in parr abundance in the following year (year 12). This peak was the result of new recruitment of age 0+ parr. Older, and larger, individuals had been killed by stranding in the previous year, so there was less pressure on the new recruits of age 0+ parr, and less density-dependent mortality of this group. This, post-hydropeaking, short-term peak in parr abundance caused a peak in smolt production several years later, followed by a peak in egg deposition several years later (year 17) when surviving adults returned from the sea to spawn (Figure 6, lower panel). In contrast, when hydropeaking was applied for an extended period of time, the perturbation pattern was simpler. That is, hydropeaking over successive years reduced recruitment into age 0+ parr over successive years, so no short-term peak in parr abundance occurred, resulting in a long-term reduction in parr abundance before a gradual recovery.

3.3 Population sensitivity to seasonal pattern of hydropeaking

Smolt production was dependent on the season when hydropeaking was applied, whether simulating with seasonally-independent (Figure 7, left panel) or seasonally-dependent stranding mortality probabilities (Figure 7, right panel). In both cases, stranding during winter and spring (weeks of year 41-20) resulted in a smaller smolt production than stranding in summer and autumn (weeks of year 21-40). Sensitivity to when hydropeaking was applied was greatest for the simulations with a seasonally-dependent stranding mortality probability for daytime hydropeaking, resulting from the greater seasonal range in stranding mortality probability for this hydropeaking regime (
Table 2).

3.4 Sensitivity analysis: stranding mortality versus density-dependent mortality

Smolt production was more sensitive to stranding mortality probability of older age groups (Figure 8a). Smolt production was relatively insensitive to fry stranding mortality probability, with no strong trend throughout the range of stranding mortalities considered (from no mortality to 100% mortality in dewatered areas) with mean annual smolt productions varying between 0.50 and 0.52 smolts 100 m^{-2}. Smolt production was slightly more sensitive to the stranding mortality probability of age 0+ parr: altering the stranding mortality probability by -50% to +50% around the baseline value caused a change in smolt production of ≈+5% (0.53 smolts 100 m^{-2}) to ≈-5% (0.49 smolts 100 m^{-2}). In contrast, smolt production was more sensitive to the stranding mortality probability of parr in the 1-4+ age group: a change in stranding mortality from -50% to +50% around the baseline values resulted in a change in smolt production of ≈+20% (0.64 smolts 100 m^{-2}) to ≈-10% (0.47 smolts 100 m^{-2}).

Smolt production was sensitive to the density-dependent mortality probability of parr (Figure 8b). For example, altering this probability by -50% to +50% around the baseline value caused a change in smolt production of ≈+30% to ≈-20%. This relationship was non-linear, with changes in the margins of the range of values tested for this parameter (at very low or very high mortality probabilities) having drastic effects on smolt production. In comparison, smolt production was relatively insensitive to the downstream migration probability of

surplus surviving parr (parr forced out of the section by the carrying capacity being exceeded, which had not experienced subsequent density-dependent mortality). That is, smolt production was less sensitive to the direction of movement (upstream or downstream) than the mortality caused by carrying capacity being exceeded.

4 Discussion

Overall, we achieved an adequate simulation of population characteristics. The underestimate of smolt production under conditions of hydropeaking (both in the initial simulation and during sensitivity analysis) may have been caused by the fact that the simulated hydropeaking regime involved a higher frequency of hydropeaking events than may have been applied in the river. The simulations were run with a strong hydropeaking regime (5 events per week throughout the year) to highlight a clear effect. We did not know the exact number of hydropeaking events applied in the river, but it is likely that the number of events applied would have been less than that simulated. There was a difference between simulated juvenile body size distribution and that observed. This may have been caused by using a growth function parameterised from data from another river using only temperature as a predictor. While growth is strongly related to temperature, other factors such as density of conspecifics (Teichert *et al*., 2010) and food availability (Arnekleiv *et al*., 2006) may affect growth. These properties will likely have differed between the river there the model was calibrated and the River Mandalselva.

Use of a mechanistic modelling approach offered the advantage that it was possible to analyse the relative effect of different parameters (for instance, fry stranding mortality versus parr stranding mortality) on hydropeaking-induced stranding on Atlantic salmon population dynamics. Additionally, the mechanistic modelling approach allowed for modelling long-term processes, involving system lag and feedback. This could not be modelled effectively using a coupled hydrodynamic-habitat model because currently available models do not include stock-recruitment processes so cannot simulate long-term population effects. However, the value of model results depends upon the presuppositions involved in model development. In this section, we therefore discuss what the IBM approach provides in terms of understanding population dynamics resulting from hydropeaking, before addressing model uncertainties, and in particular, uncertainties in the effect of stranding mortality in comparison to density-dependent mortality, which may be used to define where further research should be focused.

4.1 Population dynamics revealed by the IBM approach

The use of an IBM allowed investigation of how hydropeaking-induced stranding may affect Atlantic salmon population dynamics across all life-stages, something that would have been difficult to infer from empirical *in situ* measurements or models of single stranding events where information obtained is simply the mortality of juvenile life-stages resulting from the single event. Firstly, it was evident that the effect of stranding mortality on parr would propagate throughout the older life stages. Fewer parr resulted in fewer smolts, which in turn reduced the number of returning adults, reduced egg deposition, and thus reduced recruitment from fry into parr in future years. Therefore, the effect of stranding may be long-term. If parr spend several years in freshwater before moving to sea and then spend

several years at sea before returning to spawn, the effects of stranding on recruitment will be evident years after the last stranding event, and the population may take some time to recover even after a hydropeaking regime has been terminated. Secondly, the IBM approach enabled the exploration of potential hydropeaking-induced temporal patterns in the population dynamics that might be contrary to intuition. For example, hydropeaking for a small number of years actually caused a subsequent short-term increase in parr abundance. This was because hydropeaking reduced total parr biomass, so that small recruits in the following year experienced lower density-dependent mortality. This potential type of phenomenon could not be inferred from an empirical study, where only an instantaneous reduction in population abundance from stranding mortality would be seen.

The IBM approach also enabled investigation of hydropeaking-induced stranding mortality within the context of the main source of mortality that juvenile Atlantic salmon typically experience in rivers – density-dependent mortality. Stranding mortality reduced population abundance (and population density), so caused a consequent reduction in density-dependent mortality. Therefore, changes in density-dependent mortality may act as a negative feedback mechanism, dampening the effect of hydropeaking. Additionally, it was shown that the specific period within the year when stranding occurs is also critically important for determining overall population effects. Empirical studies have shown that mortality in single stranding events is seasonally dependent (Halleraker *et al*., 2003): for instance, hydropeaking in winter may lead to greater standing mortality than hydropeaking during summer. However, by specifying a constant stranding mortality in the model, it was still found that hydropeaking during winter had a greater effect on the population than hydropeaking during summer. This was because the main period of density-dependent mortality occurred during summer, and hydropeaking during summer could be partially compensated for by a reduction in density-dependent mortality. In winter and spring, population abundance was too low for density-dependent mortality to be occurring, so there was no possibility for a compensatory density-dependent response to stranding mortality. Therefore, stranding mortality during these seasons caused a comparatively large reduction in population abundance. It is only through an IBM approach, in which it is possible to assign specified stranding mortality probabilities, that it is possible to see a seasonal effect that is caused by the time period of stranding in respect to when density-dependent mortality occurs.

4.2 Uncertainties in modelling hydropeaking-induced stranding mortality

The act of modelling a complex environmental system involves simplification to only include those phenomena which are expected to be the most important. In the current study, potential uncertainties were introduced by (i) a fairly crude characterisation of hydropeaking events, (ii) a simple model of the fish response to down-ramping, (iii) the omission of other potential effects of hydropeaking, and (iv) the omission of potential biological influences.

Firstly, the modelling of hydropeaking-induced dewatering only characterised the main features of hydropeaking events. With regard to modelling density-dependent mortality and stranding mortality, the watercourse was modelled as a 1-D stretch, using 50 m long sections with a discharge-wetted area relationship determined at the scale of the section. In reality, the exact area dewatered will be dependent on more detailed characteristics of the channel

within the section. Following from the work of Sauterleute *et al*. (2016), our hypothesis was that the simulation of population dynamics over longitudinal reaches of 50 m in length would not be improved by using a more advanced 2-D or 3-D hydraulic model. While a 1-D approach may provide acceptable estimates of dewatering for a river with simple channel characteristics that is adequately surveyed (Casas-Mulet *et al*., 2015), a 2-D approach has the potential for better modelling of the hydraulics if high resolution data are available (Vozinaki *et al*., 2017). Also, down-ramping in the model affected the entire watercourse with the same intensity, whereas in reality, there is usually a downstream decline in the down-ramping magnitude (Hauer *et al*., 2017a). The focus of this study was on analysing how Atlantic salmon populations respond to changes in wetted width induced by hydropeaking, and the possible feedback mechanisms involved, rather than using the model as a predictive tool specifically for the River Mandalselva. As such, a crude method was used to determine wetted width as a function of discharge (dependent upon the limited data available). This would not have affected out ability to analyse how the population responded to a change in wetted area. That is, provided our model was used to analyse population responses to a change in wetted area, rather than as a predictive model for how wetted area changes according to discharge, errors resulting from the crude 1-D modelling approach will not have been an issue.

Secondly, stranding mortality within the IBM was modelled simply as the product of the dewatered area during the down-ramping cycle of the hydropeaking event (potential varying between 0, no dewatered area, and 1, all dewatered) and the assigned stranding mortality probability. However, the extent to which fish are affected by dewatering is not fully known. Increased movement in response to hydropeaking has been observed (Puffer *et al.*, 2015), and there is potential for fish to move to a deeper part of the channel on down-ramping. Inconsistencies as to how fish react to stranding may be one of the reasons that stranding effects reported in the literature have not always been consistent. For instance, Bradford *et al*. (1995) and Halleraker *et al*. (2003) reported more stranding during daytime whereas Bradford (1997) reported more stranding during night. There is potential to model this using a 2D hydrodynamic model, coupled with a 2D individual-based model. However, a model of this type that incorporates stock-recruitment relationships so that long-term population effects over multiple generations has not yet been developed.

Thirdly, hydropeaking may have a large number of potential direct and indirect effects on fish populations (Young *et al*., 2011) other than just the stranding mortality that was modelled within the IBM. Hydropeaking may be energetically costly to fish, with subsequent effects on growth (Puffer *et al*., 2015) and over-winter survival (Scruton *et al*., 2008). Dewatering parts of the channel may alter stream ecology by changing physiochemical properties such as dissolved oxygen, ionised ammonia, and turbidity. The increase in turbidity from flow fluctuation may impair fish vision, reducing prey capture success, and reduce respiratory activity through gill abrasion. Hydropeaking may also affect the benthic and insect community (Cereghino & Lavandier, 1998; Cereghino *et al*., 2002; Bruno *et al*., 2016) which may affect food webs. Finally, hydropeaking may also change the river morphology, with subsequent effects on the river's ecological characteristics (Tuhtan *et al*., 2012).

In addition to uncertainties related to hydropeaking-induced mortality, there are properties of Atlantic salmon population dynamics that are not well known. For example, density-dependent mortality is a complex issue, with the strength of the dependence depending upon the degree of interaction between conspecifics from different age groups of the same species, and potential interactions with different fish species. These interactions have not been established robustly. All parr in the IBM were pooled in terms of determining if the parr biomass exceeded parr carrying capacity, but it is feasible that there are situations where there is less interaction between different age groups, and where the use of separate age-specific density-dependent mortalities might be advisable. Another aspect that was difficult to parameterise in the IBM was density-dependent migration of Atlantic salmon juveniles: distances vary within populations, with juveniles being shown to move both upstream and downstream (Erkinaro *et al*., 1998). Additionally, multiple stranding events occurred within the weekly time-step of the IBM, with the effect of these being integrated across the time-step. Density-dependent mortality was only applied the week following the integration of multiple standing events, rather than after each individual stranding event. It is possible, therefore, that some of the fine-scale interaction between these two sources of mortality was missed. Finally, compartmentalising the watercourse into spatially-integrated sections of 50 m in length limited the ability to model fine-scale processes. For instance, a reduction in wetted area will have resulted in an increase in density-dependent mortality within the model, on the assumption that all wetted area was used. In reality, it is possible that not all of the section would have been suitable habitat, and that the relationship between changes in wetted area and density-dependent mortality in reality may be more complex.

4.3 Sensitivity of the population to stranding and non-stranding effects

When examining model sensitivity via a linear sensitivity analysis approach, parr density-dependent mortality probability (which occurred when the carrying capacity was exceeded), had a large effect on smolt production. Quantifying this parameter is difficult, and in reality the level will depend on a wide range of factors such as life-stage, time of year, flow conditions, and channel characteristics. Within the range of parameter values explored, the effect on smolt production was much greater than that for the ranges of juvenile stranding mortality probabilities established in the literature. We infer, therefore, that (with the caveat that a relatively simple sensitivity analysis approach was used) it would be prudent to achieve a better understanding of the biological uncertainties in density-dependent mortality, so that possible effects of stranding can be interpreted in the context of this uncertainty for a better management of Atlantic salmon populations in rivers experiencing hydropeaking.

5 Conclusions

Using a modelling approach (an IBM incorporating stock-recruitment so that long-term population trends could be simulated) it was possible to elucidate how hydropeaking-induced stranding mortality may affect Atlantic salmon population abundance across multiple generations. Effects of stranding on population abundance were complex, involving compensatory changes in juvenile density-dependent mortality (the main source of mortality that juvenile fishes experience in rivers). Stranding immediately preceding smoltification

caused a strong decline in smolt production, because there was less potential for a reduction in juvenile density-dependent mortality to compensate for stranding mortality. Stranding perturbed population dynamics long after the stranding. Thus, results from individual empirical experiment on stranding mortality may not necessarily be reflected in overall population effects. Smolt production was more sensitive to density-dependent mortality than stranding mortality for the range of values considered. There is a lack of knowledge on the magnitude of density-dependent mortality, so it is suggested that this area should be prioritised for future research.

Acknowledgements

This research was funded by the Research Council of Norway and the Centre for Environmental Design of Renewable Energy (CEDREN, p. no.: 193818/56) under the Centers for Environmentally Friendly Energy Research (FME) and the industry and management partners of CEDREN.

References

Arnekleiv, J. V., Finstad, A. G. & Ronning, L. (2006). Temporal and spatial variation in growth of juvenile Atlantic salmon. *Journal of Fish Biology*, *68*, 1062-1076. DOI: 10.1111/j.1095-8649.2006.00986.x

Beall, E., Dumas, J., Claireaux, D., Barriere, L. & Marty, C. (1994). Dispersal patterns and survival of Atlantic salmon (*Salmo-salar* L) juveniles in a nursery stream. *Ices Journal of Marine Science*, *51*, 1-9. DOI: 10.1006/jmsc.1994.1001

Bradford, M. J. (1997). An experimental study of stranding of juvenile salmonids on gravel ears and in sidechannels during rapid flow decreases. *Regulated Rivers-Research & Management*, *13*, 395-401. DOI: 10.1002/(sici)1099-1646(199709/10)13:5<395::aid-rrr464>3.0.co;2-l-

Bradford, M. J., Taylor, G. C., Allan, J. A. & Higgins, P. S. (1995). An experimental study of the stranding of juvenile coho salmon and rainbow trout during rapid flow decreases under winter conditions. *North American Journal of Fisheries Management*, *15*, 473-479. DOI: 10.1577/1548-8675(1995)015<0473:AESOTS>2.3.CO;2

Bruno, M. C., Cashman, M. J., Maiolini, B., Biffi, S. & Zolezzi, G. (2016). Responses of benthic invertebrates to repeated hydropeaking in semi-natural flume simulations. *Ecohydrology*, *9*, 68-82. DOI: 10.1002/eco.1611

Brunsdon, E. B., Fraser, D. J., Ardren, W. R. & Grant, J. W. A. (2017). Dispersal and density-dependent growth of Atlantic salmon (Salmo salar) juveniles: clumped versus dispersed stocking. *Canadian Journal of Fisheries and Aquatic Sciences*, *74*, 1337-1347. DOI: 10.1139/cjfas-2015-0488

Bustos, A. A., Hedger, R. D., Fjeldstad, H.-P., Alfredsen, K., Sundt, H. & Barton, D. N. (2017). Modeling the effects of alternative mitigation measures on Atlantic salmon production in a regulated river. *Water Resources and Economics*, *17*, 32-41. DOI: 10.1016/j.wre.2017.02.003

Casas-Mulet, R., Alfredsen, K., Boissy, T., Sundt, H. & Ruther, N. (2015). Performance of a one-dimensional hydraulic model for the calculation of stranding areas in hydropeaking rivers. *River Research and Applications*, *31*, 143-155. DOI: 10.1002/rra.2734

Cereghino, R., Cugny, P. & Lavandier, P. (2002). Influence of intermittent hydropeaking on the longitudinal zonation patterns of benthic invertebrates in a mountain stream. *International Review of Hydrobiology*, *87*, 47-60. DOI: 10.1002/1522-2632(200201)87:1<47::aid-iroh47>3.0.co;2-9

Cereghino, R. & Lavandier, P. (1998). Influence of hypolimnetic hydropeaking on the distribution and population dynamics of Ephemeroptera in a mountain stream. *Freshwater Biology*, *40*, 385-399. DOI: 10.1046/j.1365-2427.1998.00353.x

Chaput, G. (2012). Overview of the status of Atlantic salmon (*Salmo salar*) in the North Atlantic and trends in marine mortality. *Ices Journal of Marine Science*, *69*, 1538-1548. DOI: 10.1093/icesjms/fss013

Einum, S., Sundt-Hansen, L. & Nislow, K. H. (2006). The partitioning of density-dependent dispersal, growth and survival throughout ontogeny in a highly fecund organism. *Oikos* 113, 489-496. DOI: 10.1111/j.2006.0030-1299.14806.x

Erkinaro, J., Julkunen, M. & Niemela, E. (1998). Migration of juvenile Atlantic salmon Salmo salar in small tributaries of the subarctic River Teno, northern Finland. *Aquaculture*, *168*, 105-119. DOI: 10.1016/s0044-8486(98)00343-3

Halleraker, J. H., Saltveit, S. J., Harby, A., Arnekleiv, J. V., Fjeldstad, H. P. & Kohler, B. (2003). Factors influencing stranding of wild juvenile brown trout (*Salmo trutta*) during rapid and frequent flow decreases in an artificial stream. *River Research and Applications*, *19*, 589-603. DOI: 10.1002/rr.752

Harby, A., Alfredsen, A. K., Arnekleiv, J. V., Flodmark, L. E. W., Halleraker, J. H., Johansen, S. & Saltveit, S. J. (2004). Raske vannstandsendringer i elver - Virkninger på fisk, bunndyr og begroing. *SINTEF Teknisk Rapport*, 39.

Hauer, C., Holzapfel, P., Leitner, P. & Graf, W. (2017a). Longitudinal assessment of hydropeaking impacts on various scales for an improved process understanding and the design of mitigation measures. *Science of the Total Environment*, *575*, 1503-1514. DOI: 10.1016/j.scitotenv.2016.10.031

Hauer, C., Siviglia, A. & Zolezzi, G. (2017b). Hydropeaking in regulated rivers - From process understanding to design of mitigation measures. *Science of the Total Environment*, *579*, 22-26. DOI: 10.1016/j.scitotenv.2016.11.028

Hauer, C., Unfer, G., Holzapfel, P., Haimann, M. & Habersack, H. (2014). Impact of channel bar form and grain size variability on estimated stranding risk of juvenile brown trout during hydropeaking. *Earth Surface Processes and Landforms*, *39*, 1622-1641. DOI: 10.1002/esp.3552

Hedger, R. D., Sundt-Hansen, L. E., Forseth, T., Diserud, O. H., Ugedal, O. & Finstad, A. G. (2013a). Modelling the complete life-cycle of Atlantic salmon (*Salmo salar* L.) using a spatially explicit individual-based approach. *Ecological Modelling*, *248*, 119-129. DOI: 10.1016/j.ecolmodel.2012.10.003

Hedger, R. D., Sundt-Hansen, L. E., Forseth, T., Ugedal, O., Diserud, O. H., Kvambekk, A. S. & Finstad, A. G. (2013b). Predicting climate change effects on subarctic-Arctic populations of Atlantic salmon (*Salmo salar*). *Canadian Journal of Fisheries and Aquatic Sciences*, *70*, 159-168. DOI: 10.1139/cjfas-2012-0205

Hvidsten, N. A. (1985). Mortality of pre-smolt Atlantic salmon, *Salmo salar* L., and brown trout, *Salmo trutta* L., caused by rapidly fluctuating water levels in the regulated River

Nidelva, central Norway. *Journal of Fish Biology*, *27*, 711-718. DOI: 10.1111/j.1095-8649.1985.tb03215.x

Irvine, R. L., Oussoren, T., Baxter, J. S. & Schmidt, D. C. (2009). The effects of flow reduction rates on fish stranding in British Columbia, Canada. *River Research and Applications*, *25*, 405-415. DOI: 10.1002/rra.1172

Liebig, H., Cereghino, R., Lim, P., Belaud, A. & Lek, S. (1999). Impact of hydropeaking on the abundance of juvenile brown trout in a Pyrenean stream. *Archiv Fur Hydrobiologie*, *144*, 439-454.

Nagrodski, A., Raby, G. D., Hasler, C. T., Taylor, M. K. & Cooke, S. J. (2012). Fish stranding in freshwater systems: Sources, consequences, and mitigation. *Journal of Environmental Management*, *103*, 133-141. DOI: 10.1016/j.jenvman.2012.03.007

NASCO (2009). Protection, Restoration and Enhancement of Salmon Habitat – Focus Area Report – Norway. In *NASCO report*, p. 17: NASCO.

Niu, S. L. & Insley, M. (2013). On the economics of ramping rate restrictions at hydro power plants: Balancing profitability and environmental costs. *Energy Economics*, *39*, 39-52. DOI: 10.1016/j.eneco.2013.04.002

Puffer, M., Berg, O. K., Huusko, A., Vehanen, T., Forseth, T. & Einum, S. (2015). Seasonal Effects of Hydropeaking on Growth, Energetics and Movement of Juvenile Atlantic Salmon (*Salmo salar*). *River Research and Applications*, *31*, 1101-1108. DOI: 10.1002/rra.2801

Saltveit, S. J., Halleraker, J. H., Arnekleiv, J. V. & Harby, A. (2001). Field experiments on stranding in juvenile Atlantic salmon (*Salmo salar*) and brown trout (*Salmo trutta*) during rapid flow decreases caused byhydropeaking. *Regulated Rivers-Research & Management*, *17*, 609-622. DOI: 10.1002/rrr.652.abs

Sauterleute, J. F., Hedger, R. D., Hauer, C., Pulg, U., Skoglunde, H., Sundt-Hansen, L. E., Haakon Bakken, T. & Ugedal, O. (2016). Modelling the effects of stranding on the Atlantic salmon population in the Dale River, Norway. *Science of the Total Environment*, *573*, 574–584. DOI: 10.1016/j.scitotenv.2016.08.080

Schmutz, S., Bakken, T. H., Friedrich, T., Greimel, F., Harby, A., Jungwirth, M., Melcher, A., Unfer, G. & Zeiringer, B. (2015). Response of Fish Communities to Hydrological and Morphological Alterations in Hydropeaking Rivers of Austria. *River Research and Applications* 31, 919-930. DOI: 10.1002/rra.2795

Scruton, D. A., Pennell, C., Ollerhead, L. M. N., Alfredsen, K., Stickler, M., Harby, A., Robertson, M., Clarke, K. D. & LeDrew, L. J. (2008). A synopsis of 'hydropeaking' studies on the response of juvenile Atlantic salmon to experimental flow alteration. *Hydrobiologia* 609, 263-275. DOI: 10.1007/s10750-008-9409-x

Teichert, M. A. K., Kvingedal, E., Forseth, T., Ugedal, O. & Finstad, A. G. (2010). Effects of discharge and local density on the growth of juvenile Atlantic salmon Salmo salar. *Journal of Fish Biology*, *76*, 1751-1769. DOI: 10.1139/f10-141

Tiffan, K. F., Garland, R. D. & Rondorf, D. W. (2002). Quantifying flow-dependent changes in subyearling fall chinook salmon rearing habitat using two-dimensional spatially explicit modeling. *North American Journal of Fisheries Management*, *22*, 713-726. DOI: 10.1577/1548-8675(2002)022<0713:qfdcis>2.0.co;2

Tuhtan, J. A., Noack, M. & Wieprecht, S. (2012). Estimating Stranding Risk due to Hydropeaking for Juvenile European Grayling Considering River Morphology. *Ksce Journal of Civil Engineering*, *16*, 197-206. DOI: 10.1007/s12205-012-0002-5

Ugedal, O., Larsen, B. M., Forseth, T. & Johnsen, B. O. (2006). The production capacity for Atlantic salmon and estimated losses due to hydropower regulation in the River Mandalselva. *NINA Report* 146, 44.

Vozinaki, A. E. K., Morianou, G. G., Alexakis, D. D. & Tsanis, I. K. (2017). Comparing 1D and combined 1D/2D hydraulic simulations using high-resolution topographic data: a case study of the Koiliaris basin, Greece. *Hydrological Sciences Journal*, *62*, 642-656. DOI: 10.1080/02626667.2016.1255746

Young, P. S., Cech, J. J. & Thompson, L. C. (2011). Hydropower-related pulsed-flow impacts on stream fishes: a brief review, conceptual model, knowledge gaps, and research needs. *Reviews in Fish Biology and Fisheries*, *21*, 713-731. DOI: 10.1007/s11160-011-9211-0

Tables

Table 1. Relationship between discharge, Q (m^3 s^{-1}), and wetted width, W (m), established from a polynomial regression fitted to the hydraulic model output.

Channel type	Discharge (m^3 s^{-1}) wetted width (m) relationship	Discharge range
'U'-shaped	$W = 11.24Q$	$Q < 5$
	$W = 71.93 - \frac{250.12}{Q} + \frac{1587.52}{Q^2} - \frac{3648.27}{Q^3}$	$5 < Q < 70$
	$W = 67.66 + 0.02Q$	$Q \geq 70$
Intermediate	$W = 4.15Q$	$Q < 15$
	$W = 78.07 - \frac{256.45}{Q} + \frac{2404.09}{Q^2} - \frac{31635.11}{Q^3}$	$15 < Q < 120$
	$W = 73.99 + 0.02Q$	$Q >= 120$
'V'-shaped	$W = 4.28Q$	$Q < 17$
	$W = 114.45 - \frac{476.70}{Q} - \frac{14539.50}{Q^2} + \frac{180507.97}{Q^3}$	$17 < Q < 155$
	$W = 105.08 + 0.04Q$	$Q \geq 150$

Table 2. Seasonal stranding mortality probabilities applied for hydropeaking during night-time and daytime.

Season	Weeks of year	Night-time			Daytime		
		Fry	0+ parr	1-4+ parr	Fry	0+ parr	1-4+ parr
Spring	9-21	0.9	0.20	0.15	0.9	0.20	0.15
Summer	22-34	0.9	0.10	0.05	0.9	0.10	0.05
Autumn	35-48	0.9	0.10	0.05	0.9	0.10	0.05
Winter	48-8	0.9	0.15	0.10	0.9	0.40	0.40

Table 3. Parameters explored in sensitivity analysis. Parameters are (i) stranding mortality probability of fry (S_{fry}); (ii) stranding mortality probability of age 0+ parr (S_{0+parr}); (iii) stranding mortality probability of age 1-4+ parr ($S_{1-4+parr}$); (iv) density-dependent mortality probability of parr (D_{parr}); and (v) probability of a surviving individual migrating downstream (M_{parr}).

Parameter being analysed	Baseline value	Range	Value of other parameters				
			S_{fry}	S_{0+parr}	$S_{1-4+parr}$	D_{parr}	M_{parr}
S_{fry}	0.90	(0.00, 0.10, ... 1.00)	NA	0.2	0.2	0.5	1.0
S_{0+parr}	0.20	(0.10, 0.12, ... 0.30)	0.9	NA	0.2	0.5	1.0
$S_{1-4+parr}$	0.20	(0.10, 0.12, ... 0.30)	0.9	0.2	NA	0.5	1.0
D_{parr}	0.50	(0.05, 0.1, ... 1.0)	0.9	0.2	0.2	NA	1.0
M_{parr}	1.0	(0.5, 0.55, ... 1.0)	0.9	0.2	0.2	0.5	NA

Figure captions

Figure 1. Sources of mortality within the IBM: density-dependent mortality for parr within a section (left panel); and hydropeaking-induced stranding mortality for parr within a part of the section dewatered during down-ramping (right panel). In both panels, the thick line shows the relationship between the population at time T and the population at time T+1, the dashed line shows the relationship for an equivalent population for time T and time T+1, and the solid arrows show how a population level at time T is transferred into a population level at time T+1. In the left panel, the dotted arrow shows the total of biomass of parr that is not recruited within the section, some of which will move to another section (through parr migration) and some of which will be removed via density dependent mortality, and K_{sec} shows the carrying capacity of the section (dependent on the weekly wetted area).

Figure 2. Simulated and observed population characteristics: parr abundance (week of year = 52) (left panel); and parr body length (right panel). Observed characteristics were derived from data acquired by the Norwegian Environment Agency. The simulated population was generated under conditions of five hydropeaking events per week.

Figure 3. Parr abundance (week of year = 52) and annual smolt production under conditions of no hydropeaking (left panels) and hydropeaking applied five days per week (right panels).

Figure 4. Weekly parr abundance and total parr mortality under conditions of no hydropeaking (left panels) and hydropeaking applied five days per week (right panels) for year-of-simulation 11, the first year after model “burn-in”.

Figure 5. Weekly parr abundance (upper panel) and total parr mortality (lower panel) under conditions of hydropeaking applied five days per week for the first six years after hydropeaking is applied. The beginning of the initial year of hydropeaking (year 11) is indicated by a vertical dashed line.

Figure 6. Effect of number of years of hydropeaking on parr abundance (week of year = 52) (upper panel) and egg production (lower panel). The beginning of the initial year of hydropeaking (year 11) is indicated by a vertical dashed line.

Figure 7. Effect of seasonal pattern of hydropeaking on smolt production under conditions of seasonally-independent stranding mortality probability (S_{fry} = 0.9; S_{parr} = 0.2) (left panel) and seasonally-dependent stranding mortality probability (right panel). Seasonally-dependent stranding mortalities are shown in Table 2.

Figure 8. Sensitivity of smolt production to (a) stranding mortality probability of fry, age 0+ parr, and age 1-4+ parr, and (b) parr density-dependent mortality probability and parr downstream migration probability. Changes in smolt production are calculated as changes from the baseline value (Table 3). Baseline values are shown by the vertical dashed line.

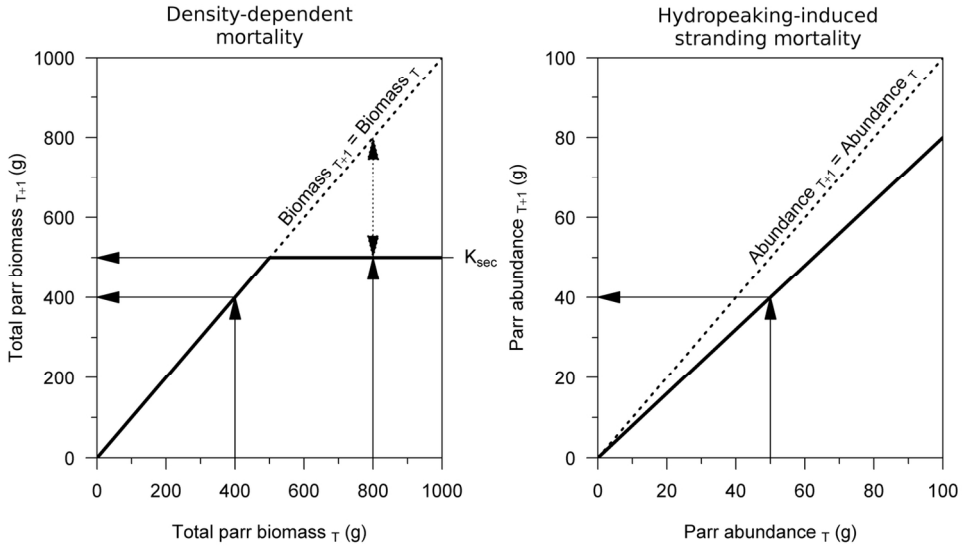

Figure 1. Sources of mortality within the IBM: density-dependent mortality for parr within a section (left panel); and hydropeaking-induced stranding mortality for parr within a part of the section dewatered during down-ramping (right panel). In both panels, the thick line shows the relationship between the population at time T and the population at time T+1, the dashed line shows the relationship for an equivalent population for time T and time T+1, and the solid arrows show how a population level at time T is transferred into a population level at time T+1. In the left panel, the dotted arrow shows the total of biomass of parr that is not recruited within the section, some of which will move to another section (through parr migration) and some of which will be removed via density dependent mortality, and Ksec shows the carrying capacity of the section (dependent on the weekly wetted area).

135x80mm (300 x 300 DPI)

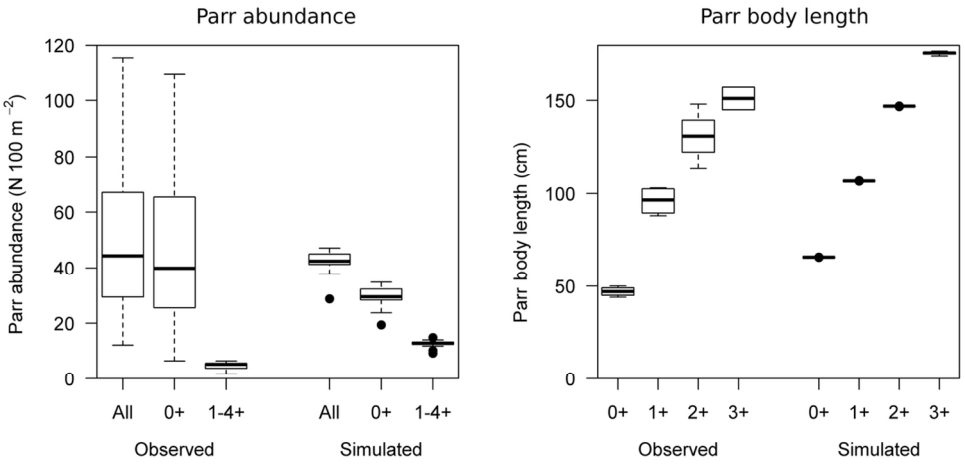

Figure 2. Simulated and observed population characteristics: parr abundance (week of year = 52) (left panel); and parr body length (right panel). Observed characteristics were derived from data acquired by the Norwegian Environment Agency. The simulated population was generated under conditions of five hydropeaking events per week.

114x57mm (300 x 300 DPI)

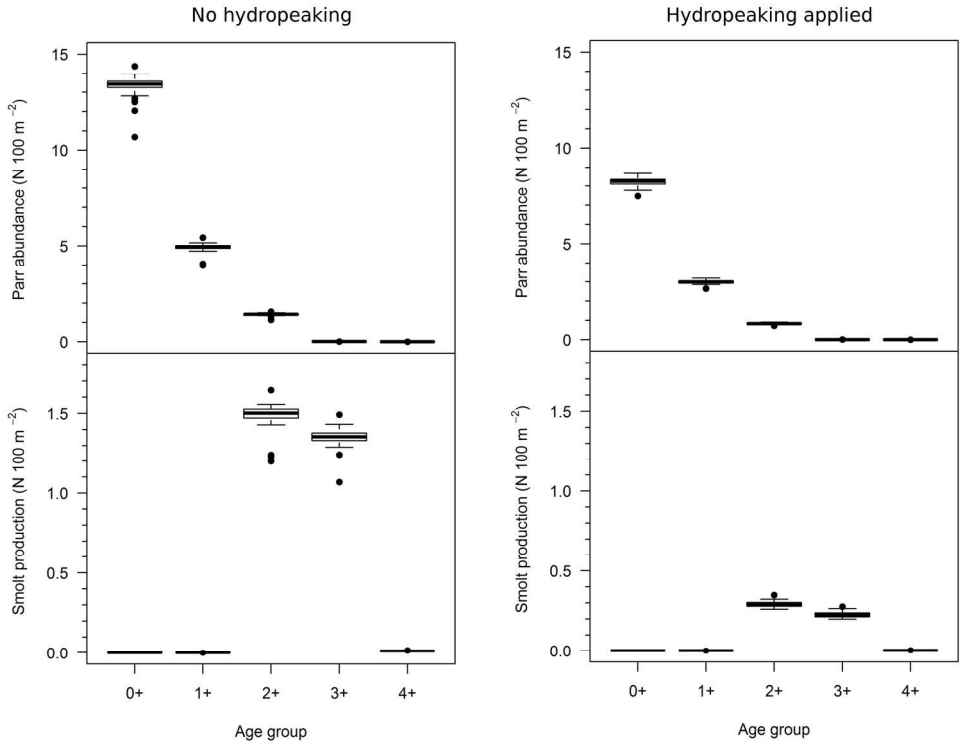

Figure 3. Parr abundance (week of year = 52) and annual smolt production under conditions of no hydropeaking (left panels) and hydropeaking applied five days per week (right panels).

172x133mm (300 x 300 DPI)

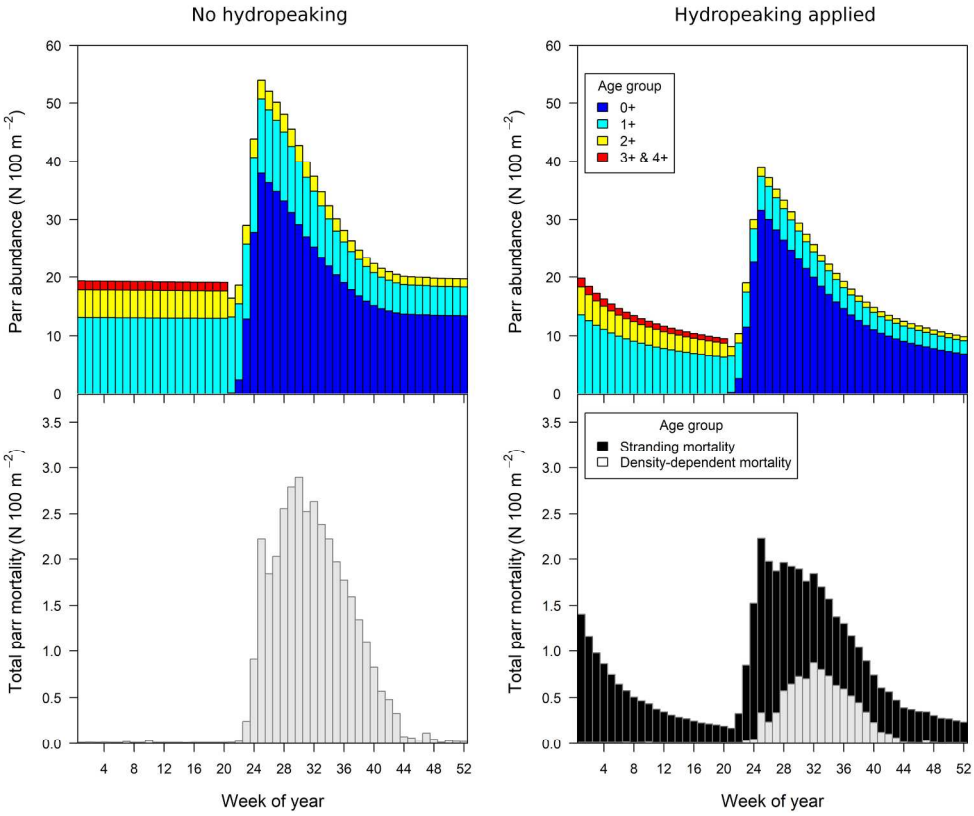

Figure 4. Weekly parr abundance and total parr mortality under conditions of no hydropeaking (left panels) and hydropeaking applied five days per week (right panels) for year-of-simulation 11, the first year after model "burn-in".

219x190mm (300 x 300 DPI)

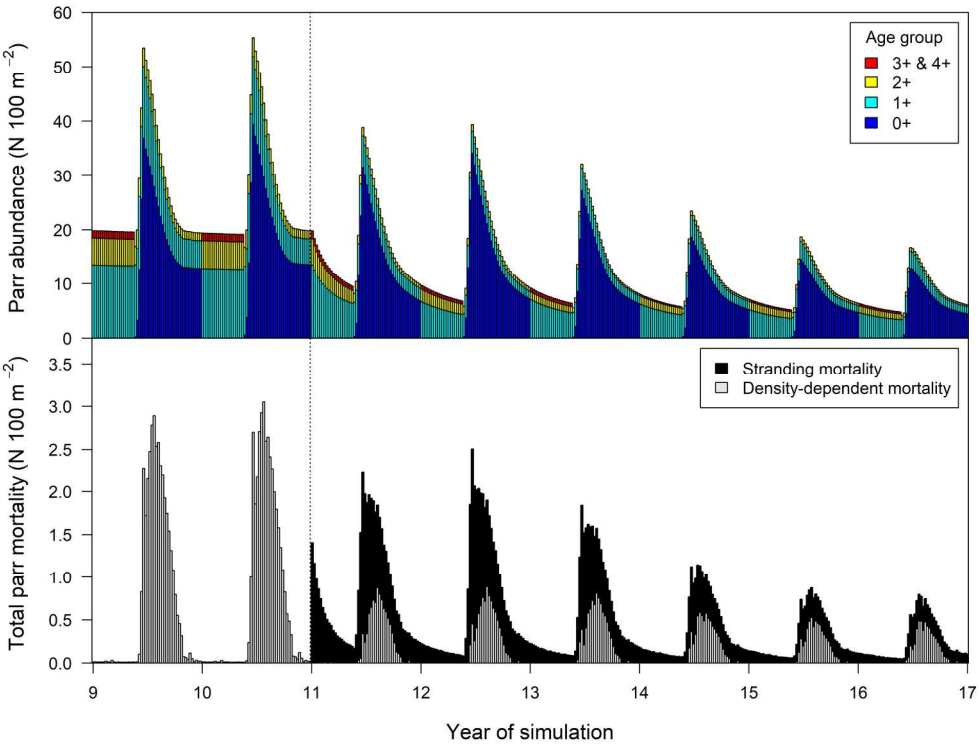

Figure 5. Weekly parr abundance (upper panel) and total parr mortality (lower panel) under conditions of hydropeaking applied five days per week for the first six years after hydropeaking is applied. The beginning of the initial year of hydropeaking (year 11) is indicated by a vertical dashed line.

203x162mm (300 x 300 DPI)

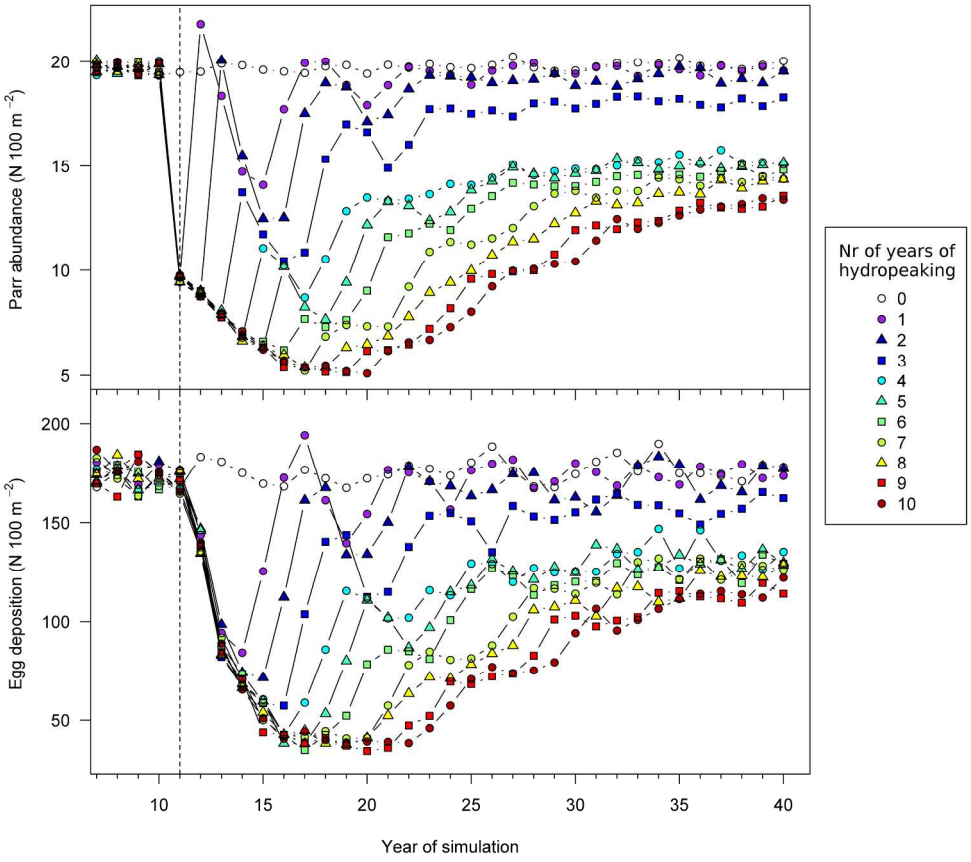

Figure 6. Effect of number of years of hydropeaking on parr abundance (week of year = 52) (upper panel) and egg production (lower panel). The beginning of the initial year of hydropeaking (year 11) is indicated by a vertical dashed line.

227x209mm (300 x 300 DPI)

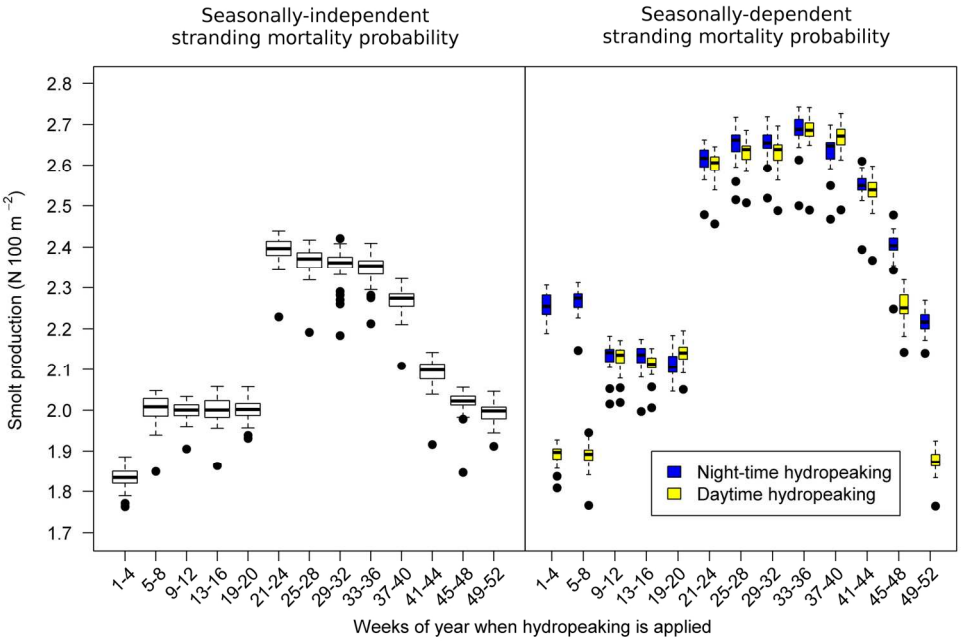

Figure 7. Effect of seasonal pattern of hydropeaking on smolt production under conditions of seasonally-independent stranding mortality probability (Sfry = 0.9; Sparr = 0.2) (left panel) and seasonally-dependent stranding mortality probability (right panel). Seasonally-dependent stranding mortalities are shown in Table 2.

160x109mm (300 x 300 DPI)

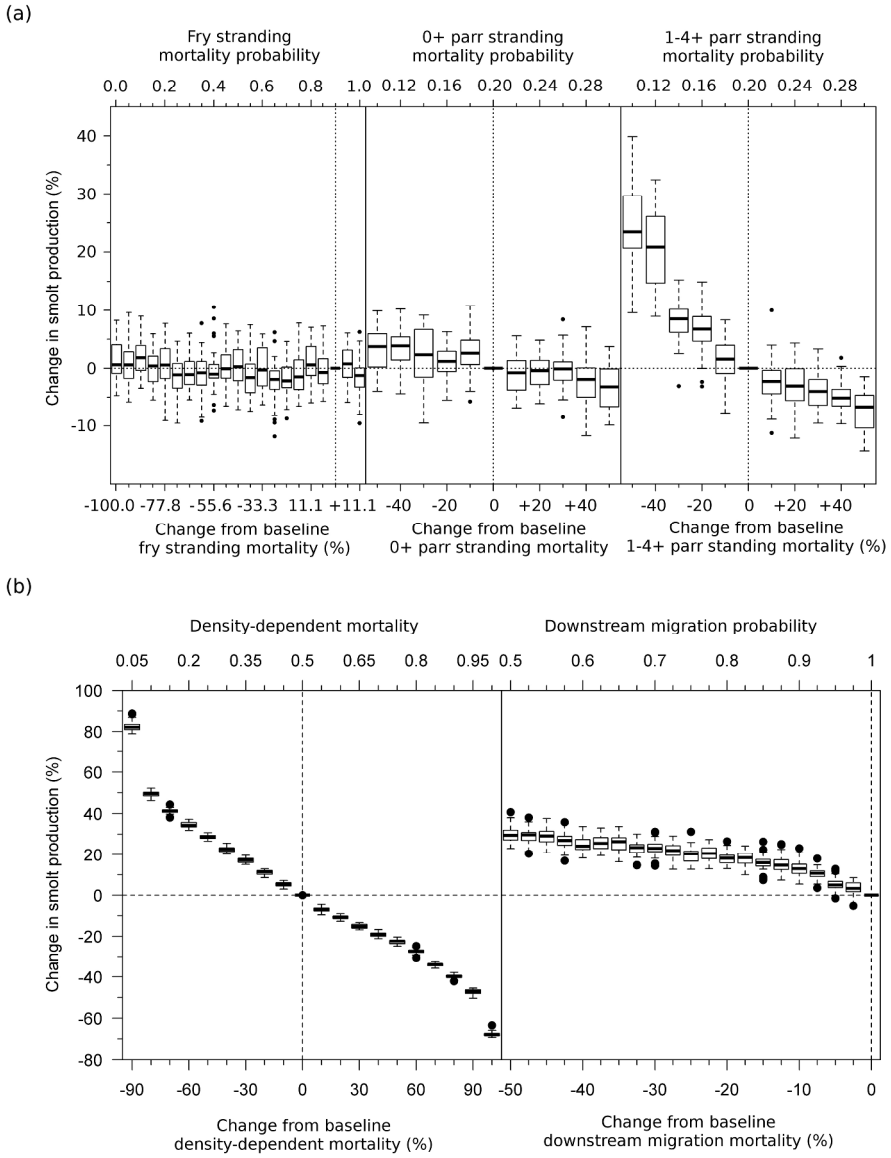

Figure 8. Sensitivity of smolt production to (a) stranding mortality probability of fry, age 0+ parr, and age 1-4+ parr, and (b) parr density-dependent mortality probability and parr downstream migration probability. Changes in smolt production are calculated as changes from the baseline value (Table 3). Baseline values are shown by the vertical dashed line.

302x391mm (300 x 300 DPI)